ISBN: 978-3-95450-231-8 ISSN: 2673-5490 doi: 10.18429/JACoW-IPAC2023-TUPL180

# A START-TO-END OPTIMISATION OF CLEAR FOR AN INVERSE COMPTON SCATTERING EXPERIMENT, USING RF-TRACK

V. Mușat*[1], A. Latina, A. Malyzhenkov, A. Aksoy, CERN, Geneva, Switzerland
[1] also at JAI, University of Oxford, Oxford, UK

*Abstract*

The CERN Linear Electron Accelerator for Research (CLEAR) has been operating as a user facility since 2017, providing beams for various experiments. This paper describes a start-to-end optimisation of the CLEAR beamline as a driver for X-ray generation through inverse Compton scattering. The novel particle tracking code RF-Track was used to simulate the electron beam from the bunch generation at the cathode up to the interaction with a laser beam. Figures of merit of the scattered photon beam were computed in RF-Track, and optimised by tuning the beam parameters at injection and quadrupole strengths across the beamline. The aim of the optimisation was to maximise the scattered photon flux, and minimise the effects from static and dynamic imperfections. The start-to-end model of the CLEAR beamline was used to derive the impact of jitter on flux.

## INTRODUCTION

Recent advancements in the average power of commercial lasers have led to a resurgence in the R&D of Inverse Compton scattering (ICS) sources as a compact alternative to synchrotrons. In particular, the energy tunability of ICS sources can be exploited to generate high-intensity gamma beams, which can be used for various applications, including protein crystallography [1], nuclear resonance fluorescence [2], or tomography, such as K-edge subtraction [3, 4].

ICS sources based on storage rings have been extensively used due to their high repetition rate [5–7]. However, besides a significant footprint, these sources are also limited by a large emittance, which decreases the average brilliance of the scattered photon beam. Sources based on linear accelerators can offer high-quality beams for pulsed operation [8–10] in considerably smaller facility sizes. The low repetition rate of linacs can be compensated by using a burst mode-operated Fabry-Perot cavity, where Joule-level laser effective energies are stored [11].

Linac-based ICS sources can benefit from developments in high gradient acceleration and high repetition rate injectors developed, for example, in the context of the Compact Linear Collider (CLIC) [12].

## THE CLEAR BEAMLINE

The CLEAR facility provides high-quality electron beams for activities comprising R&D on accelerator components for current and future accelerators, electron-based irradiation, and novel accelerating technologies [13, 14].

### *Electron Beam Parameters*

The CLEAR linac accelerates electrons up to 200 MeV. The facility can provide bunches with a length from 0.1 ps to 10 ps and charge from 5 pC to 3 nC. The train repetition rate varies from 0.83 to 10 Hz. The maximum total pulse charge is 30 nC. The photoinjector laser sets the bunch spacing to 1.5 GHz and can be increased to 3 GHz through an optical double pulse system. The relative energy spread of the electron bunch is under 0.2% RMS.

### *Laser Beam Parameters*

In the first phase of the ICS experiment, the photoinjector would provide the laser beam. This simplifies the temporal matching with the electron beam. The laser wavelength is 1047 nm, with a pulse length of 4.7 ps, a burst repetition rate of 10 Hz, and a micropulse repetition rate of 1.5 GHz. The micropulse energy ranges from 10 µJ to 15 µJ. Given 150 incident pulses, the burst energy becomes 2.3 mJ, and the average power 23 mW.

### *Interaction Region*

Considering the linear Compton regime with round Gaussian laser and electron intensity distributions and neglecting the hourglass effect, the number of photons generated through ICS in a bunch crossing is

$$N_\gamma = \sigma_T \frac{N_e N_{\text{laser}} \cos(\phi/2)}{2\pi\sigma_y \sqrt{\sigma_x^2 \cos^2(\phi/2) + \sigma_z^2 \sin^2(\phi/2)}}, \quad (1)$$

where $\sigma_T$ is the Thomson cross section, $N_e$ is the number of electrons in a bunch, $N_{\text{laser}}$ is the number of laser photons in a pulse, $\phi$ is the crossing angle between the laser and electron beam, and $\sigma_i$ with $i = x, y, z$ is the convolution of the electron and laser transverse and longitudinal size at the interaction point (IP) [15].

To maximise the outgoing flux from Eq. (1), one needs to design a source with strongly focused head-on collisions of high-density electron and laser pulses. To achieve this, the relevant electron beam parameters need to be optimised at injection, and the quadrupole strengths tuned to allow for a small waist at the IP. Optimising the CLEAR beamline required software capable of tracking the electron beam through a custom set-up and simulating ICS.

## RF-TRACK SIMULATION OF ICS

A start-to-end simulation of the CLEAR beamline was performed using RF-Track [16]. RF-Track is a tracking code developed at CERN to simulate beam transport under the simultaneous effect of space-charge forces and wakefields.

* vlad.musat@cern.ch

ISBN: 978-3-95450-231-8 ISSN: 2673-5490 doi: 10.18429/JACoW-IPAC2023-TUPL180

Linear ICS has been recently implemented and benchmarked against CAIN [17], a standard simulation code of ICS [18]. In RF-Track, the beam can be tracked from the cathode to the interaction point, where the ICS effect is computed. The scattered photon beam is then tracked up to the detector's location, where its figures of merit are evaluated. The simulation is performed in one pass from the cathode to the out-coming X-rays. Such a start-to-end simulation also allowed for studying the flux sensitivity to various sources of jitter.

The normalised beam emittance and the relative energy spread of the electron bunch are fixed at injection. Since these two parameters contribute to the quality of the scattered photon beam, a realistic simulation, based on the field maps of the CLEAR photoinjector and travelling wave structures, was implemented in the RF-Track model. At high bunch charge, beam loading effects in the RF gun and the linac become relevant. A beam-loading module has been developed in RF-Track to include these effects [19, 20].

Parameters such as the RF phase, the gradient, and the laser spot size on the photoinjector cathode were tuned to minimise emittance and energy spread at the end of the injector. This allowed for an increase in the average brilliance and a decrease in the bandwidth of the scattered photon beam.

To optimise the electron beam parameters at the interaction point, a model of the CLEAR optics was implemented in RF-Track. Using the simplex algorithm with an appropriate merit function, the quadrupole strengths were tuned to reduce the beam size and obtain a waist at the IP. To avoid beam loss from the interaction of the electron beam with the beam pipe walls, additional weighting was introduced to limit the maximum electron beam size to 10% of the beam pipe aperture. The limit was applied from the linac exit to the last dipole, after which the electron beam is separated from the scattered photon beam, and sent to the beam dump. The IP coordinates were chosen based on the available focusing power and the impact of the beam jitter on the scattered photon flux.

## BEAM PARAMETERS AT INJECTION

The optimisation of the CLEAR beamline began with the choice of beam parameters at injection. The optimisation of the linac parameters allowed for a normalised emittance of 12 mm mrad and an energy spread of 2‰ at the start of the first quadrupole triplet. To maximise the number of electrons per bunch from Eq. (1), the bunch charge was increased to 1 nC. Simulations showed that a further increase in bunch charge led to a saturation of the photon flux. A larger bunch charge corresponds to an increase in emittance under space charge effects. This leads to a weak focusing and a larger spot size at the IP. Additionally, previous laser wire studies of the CLEAR injector showed that using a bunch charge over 1 nC led to a significantly larger background in the ICS photon detector [21]. Given a total pulse charge of 30 nC at CLEAR, the number of electron bunches per train was maximised to 30. To match the longitudinal distribution of the incident laser pulse, the bunch length was set to 2 ps. The laser micropulse energy was increased to 15 µJ, which maximised the number of photons per laser pulse. A summary of the electron and laser parameters is given in Table 1.

Head-on collisions were implemented by minimising the crossing angle to 0°. Simulations showed that an increase in $\phi$ to 5° leads to a loss in flux of 40%. In linac-based ICS sources, head-on collisions can be achieved by using parabolic mirrors with drilled holes to allow for the passage of the electron beam [8].

Table 1: Parameters of the Electron Beam, Laser, and Scattered Photon Beam Obtained from the Optimisation

| Parameter | Units | Value |
|---|---|---|
| Beam energy, $E$ | MeV | 200 |
| Bunch charge, $Q$ | nC | 1 |
| Number of bunches per train | | 30 |
| Bunch length, $\sigma_z$ | ps | 2 |
| Energy spread, | ‰ | 2 |
| Normalised emittance, $\epsilon_{x,y}$ | mm mrad | 12 |
| Wavelength, $\lambda$ | nm | 1047 |
| Pulse energy, $\mathcal{E}_0$ | µJ | 15 |
| Pulse length | ps | 4.7 |
| Waist size, $w_0$ | µm | 50 |
| Photon energy, $E$ | keV | 715 |
| Total flux | ph/s | $9 \times 10^5$ |
| Flux in a 1.5 mrad cone | ph/s | $4 \times 10^5$ |
| Bandwidth in a 1.5 mrad cone | % | 9.4 |
| Spot size on detector | mm | 3 |

## QUADRUPOLE FOCUSING AT THE IP

The tracking of an electron bunch beam size through the optimised quadrupoles at CLEAR is shown in Fig. 1. The location of the IP was set after the third quadrupole triplet. This placement allowed for a strong final focusing and a minimised impact on the scattered photons flux from the jitter. The distance from the IP to the detector was minimised to 3.7 m.

A horizontal and vertical electron beam size of 86 µm and 26 µm was obtained at the interaction point. The electron beam size was kept to a value lower than 10% of the beam pipe radius, except at the exit of the quadrupole doublet. This might lead to the production of secondary radiation, which can be mitigated by either scraping the electron beam with a set of collimators or installing polyethylene boards around the X-ray beamline, attenuating the secondary neutron radiation and enabling a clear path for the scattered photons [10]. A summary of the gamma-ray parameters is given in Table 1. The ICS photon spectrum through a 1.5 mrad aperture was computed in Fig. 2, with the Compton edge at 715 keV.

ISBN: 978-3-95450-231-8 ISSN: 2673-5490 doi: 10.18429/JACoW-IPAC2023-TUPL180

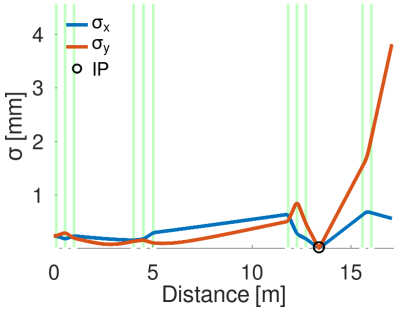


Figure 1: Tracking of the electron beam size (sigma) along the CLEAR beamline. The position of the quadrupoles is marked in green. The interaction point is circled in black.

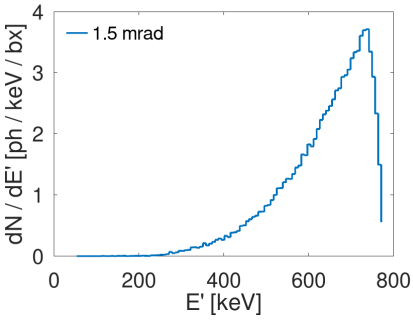


Figure 2: Scattered photon spectrum in a 1.5 mrad cone. Here, 'bx' denotes bunch crossing. The Compton edge is 715 keV.

## IMPACT OF BEAM JITTER ON FLUX

The RF-Track model of CLEAR was used to evaluate the impact of beamline jitter on the scattered photon flux in a 1.5 mrad cone. The jitter amplitudes reported at CLEAR comprise an energy jitter of 1%, a timing jitter of 300 fs, a position (angle) jitter of 10% of the beam size (divergence), a magnet displacement jitter of 1 µm, and a bunch charge jitter of 1%. A realistic estimate of the scattered photon flux was obtained by implementing all the sources of jitter into the RF-Track model. This was done by randomly varying the quantity of jitter from each source with respect to its amplitude and tracking an electron bunch through the modified beamline.

After a thousand runs, where each run is equivalent to one bunch crossing, the distribution of the change in flux through a 1.5 mrad cone due to jitter was calculated with respect to the nominal value, as shown in Fig. 3. These simulations showed that jitter in the beam energy has the most significant impact on flux. This is likely due to chromatic effects introduced by the quadrupoles preceding the IP. The simulations also showed that an energy jitter with an amplitude less than 0.25% would be required to keep changes in flux under 10%. A gamma distribution was used to fit the histogram in Fig. 3, and the mean and $\sigma$ of the flux in a 1.5 mrad cone were determined to be $4 \times 10^5 \pm 5\%$ ph/s.

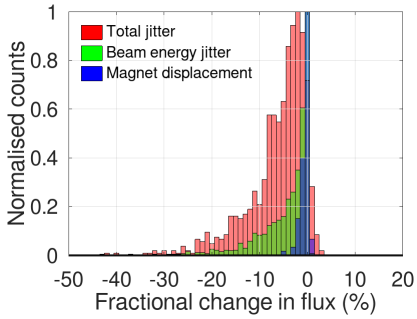


Figure 3: Histograms of the flux sensitivity for the total, beam energy, and magnet displacement jitter. Counts were normalised to the maximum bin height. The fractional change in flux was defined relative to the nominal value.

## FURTHER WORK

The optimisation of the CLEAR beamline was performed as a prerequisite for an eventual ICS experiment at the user facility. Most of the results obtained, including the photon spectrum and flux sensitivity to jitter, can be experimentally determined and benchmarked against the RF-Track simulation.

This paper was focused on the optimisation of the electron beam for ICS, however, later stages of the experiment will require the design of a burst mode-operated Fabry-Perot cavity, which will allow for a significant increase in flux. A preliminary study indicated that increasing the number of electron bunches per train to 150 will produce a maximum effective gain in the cavity of 116, maximising the effective laser energy and scattered photon flux.

The experimental apparatus will comprise an inorganic scintillator, which will detect the outgoing photons, and an interaction chamber housing the alignment equipment and optical mirrors, which will focus the laser beam at the IP. A GEANT4 [22] simulation of the detector is being developed to determine the expected signal produced by the on-detector gamma beam. This result will be used to identify background sources of radiation and reduce the detector signal-to-noise ratio.

## CONCLUSION

An optimisation of the electron beamline at the CLEAR user facility was computed in RF-Track for an inverse Compton scattering experiment. The electron and laser beam parameters were chosen to maximise the scattered photon flux. The magnetic strength of the quadrupoles was tuned to ensure a small beam size at the IP and avoid scraping of the beam pipe walls. A bunch satisfying the required conditions was tracked through the set-up, and figures of merit were determined for the scattered photon beam. The implementation of the full beamline in RF-Track allowed for determining the impact of jitter on the scattered photon flux. The sensitivity study performed showed that a photon flux in a 1.5 mrad cone of $4 \times 10^5 \pm 5\%$ ph/s can be obtained.

ISBN: 978-3-95450-231-8 ISSN: 2673-5490 doi: 10.18429/JACoW-IPAC2023-TUPL180

# REFERENCES


[1] J. Abendroth *et al.*, "X-ray structure determination of the glycine cleavage system protein H of Mycobacterium tuberculosis using an inverse Compton synchrotron X-ray source," *J. Struct. Funct. Genomics*, vol. 11, no. 1, pp. 91–100, 2010. doi:10.1007/s10969-010-9087-6

[2] R. Hajima, T. Hayakawa, N. Kikuzawa, and E. Minehara, "Proposal of nondestructive radionuclide assay using a high-flux gamma-ray source and nuclear resonance fluorescence," *J. Nucl. Sci. Technol.*, vol. 45, no. 5, pp. 441–451, 2008. doi:10.1080/18811248.2008.9711453

[3] S. Kulpe *et al.*, "K-edge subtraction imaging for coronary angiography with a compact synchrotron X-ray source," *PLoS ONE*, vol. 13, no. 12, 2018. doi:10.1371/journal.pone.0208446

[4] S. Kulpe *et al.*, "K-edge Subtraction Computed Tomography with a Compact Synchrotron X-ray Source," *Scientific Reports*, vol. 9, no. 1, 2019. doi:10.1038/s41598-019-49899-z

[5] R. Loewen, "A compact light source: Design and technical feasibility study of a laser-electron storage ring x-ray source," no. SLAC-R-632, 2004. doi:10.2172/826755

[6] K. Dupraz *et al.*, "The ThomX ICS source," *Physics Open*, vol. 5, 2020. doi:10.1016/j.physo.2020.100051

[7] H. Ogawa, N. Sei, and K. Yamada, "Asymmetric two-bunch operation of free-electron laser and generation of inverse Compton photons," *Phys. Lett. A*, vol. 376, no. 12-13, pp. 1171–1175, 2012. doi:10.1016/j.physleta.2012.02.023

[8] Y. Du *et al.*, "Generation of first hard X-ray pulse at Tsinghua Thomson Scattering X-ray Source," *Rev. Sci. Instrum.*, vol. 84, no. 5, 2013. doi:10.1063/1.4803671

[9] L. Faillace *et al.*, "Status of compact inverse Compton sources in Italy: BriXS and STAR," 2019. doi:10.1117/12.2531168

[10] P. Niknejadi *et al.*, "Free-electron laser inverse-Compton interaction x-ray source," *Phys. Rev. Accel. Beams*, vol. 22, no. 4, 2019. doi:10.1103/PhysRevAccelBeams.22.040704

[11] P. Favier *et al.*, "Optimization of a Fabry-Perot cavity operated in burst mode for Compton scattering experiments," *Phys. Rev. Accel. Beams*, vol. 21, no. 12, 2018. doi:10.1103/PhysRevAccelBeams.21.121601

[12] P. Burrows *et al.*, *The Compact Linear Collider (CLIC) - 2018 Summary Report*, P. Burrows, Ed. 2018, vol. 2. doi:10.23731/CYRM-2018-002

[13] R. Corsini *et al.*, "First Experiments at the CLEAR User Facility," in *Proc. IPAC'18*, Vancouver, Canada, Apr.-May 2018, pp. 4066–4069. doi:10.18429/JACoW-IPAC2018-THPMF014

[14] K. N. Sjobak *et al.*, "Status of the CLEAR Electron Beam User Facility at CERN," in *Proc. IPAC'19*, Melbourne, Australia, May 2019, pp. 983–986. doi:10.18429/JACoW-IPAC2019-MOPTS054

[15] G. A. Krafft and G. Priebe, "Compton Sources of Electromagnetic Radiation," *Rev. Accel Sci. Technol.*, vol. 03, no. 01, 2010. doi:10.1142/S1793626810000440

[16] A. Latina, "RF-Track Reference Manual," CERN, Tech. Rep., 2020. doi:10.5281/zenodo.3887085

[17] V. Mușat, A. Latina, and G. D'Auria, "A High-Energy and High-Intensity Inverse Compton Scattering Source Based on CompactLight Technology," *Photonics*, vol. 9, no. 5, p. 308, 2022. doi:10.3390/photonics9050308

[18] P. Chen, G. Horton-Smith, T. Ohgaki, A. W. Weidemann, and K. Yokoya, "CAIN: Conglomérat d'ABEL et d'Interactions Non-linéaires," *Nucl. Instrum. Meth. Phys. Res. Sect. A*, vol. 355, no. 1, 1995. doi:10.1016/0168-9002(94)01186-9

[19] J. O. Herrador, D. E. Pereira, N. Fuster, B. Gimeno, and A. Latina, "Beam Loading Simulation for Relativistic and Ultrarelativistic Beams in the Tracking Code RF-Track," in *Proc. LINAC'22*, Liverpool, UK, 2022, pp. 569–572. doi:10.18429/JACoW-LINAC2022-TUPORI13

[20] J. Olivares Herrador, A. Latina, N. Fuster, B. Gimeno, and D. Esperante, "Beam loading effects in standing-wave RF Structures and their implementation into the Particle Tracking Code RF-Track," presented at IPAC'23, Venice, Italy, 2023, paper WEPL152, this conference.

[21] J. Bosser *et al.*, "Laser Wire Scanner Development on CTF II," in *Proc. LINAC'02*, Gyeongju, Korea, Aug. 2002, pp. 326–328. https://jacow.org/l02/papers/TU411.pdf

[22] S. Agostinelli *et al.*, "Geant4—a simulation toolkit," *Nucl. Instrum. Meth. Phys. Res. Sect. A*, vol. 506, no. 3, pp. 250–303, 2003. doi:10.1016/S0168-9002(03)01368-8